Mitigating optical losses in crystalline silicon thin-film solar cells on glass

David Eisenhauer, Bernd Rech, and Christiane Becker

Helmholtz-Zentrum Berlin für Materialien und Energie GmbH, 12489 Berlin, Germany

***Abstract* — Liquid phase crystallized silicon thin-film solar cells on glass provide efficiencies up to 14.2 %. While open-circuit voltage and fill factor are already comparable to wafer-based devices, short-circuit current density is reduced due to incomplete light absorption. This paper analyzes the losses of current device designs in experiment and one-dimensional simulations, revealing the low absorber thickness of 15-20 µm as well as the planar glass-silicon interface as the main cause of non-absorption. Interface textures, in particular a sinusoidal texture and a smooth anti-reflective three-dimensional (SMART) texture, are discussed concerning their potential to mitigate these losses, allowing to reduce losses at the glass-silicon interface by at least 40% relative. Taking the electronic interface quality into account, the SMART texture is identified as the most promising texture for light management in liquid phase crystallized silicon thin-film solar cells on glass.**

***Index Terms* — silicon, thin-film solar cells, light management, absorption enhancement.**

I. Introduction

Liquid phase crystallization (LPC) of 15 – 20 µm thick silicon layers is a promising technology for thin-film solar cells with both, high efficiencies and low costs. Recently, a power conversion efficiency of 14.2 % could be demonstrated [1], whereby the open-circuit voltage of 654 mV and fill factor of 75 % are already close to values achieved of record devices for wafer-based high-performance multi-crystalline silicon solar cells [2]. The lower efficiency mainly results from a reduced short-circuit current density caused by optical losses. These losses arise from the more than tenfold lower absorber thickness of the LPC silicon solar cell and high reflectance at planar interfaces. Reducing the losses requires improved light management in order to increase the short-circuit current density in LPC silicon thin-film solar cells on glass and in order to draw closer to efficiencies of wafer-based approaches. One method that has proven to yield an increased light in-coupling into the absorber is the introduction of textures at the glass-silicon interface, both using random [3]–[5] and periodic [6]–[8] structures. However, a trade-off between improved optical properties from pronounced texturing and deteriorated electronic material quality due to texture-induced interface defects was identified [6], posing further requirements for suitable light management schemes. Texturing methods that allowed both, improving light in-coupling while preserving an electronic material quality comparable to planar LPC devices include a sinusoidal texture [7] and a smooth anti-reflective three-dimensional (SMART) texture [8], as demonstrated by maximum open-circuit voltages of 618 mV and 649 mV, respectively.

In this contribution, we discuss the optical losses of the state-of-the-art device design of liquid phase crystallized silicon thin-film solar cells on glass with a planar glass-silicon interface in experiment and one-dimensional simulations. Based on these results, the potential gains from glass-silicon texturing are presented considering both optical properties as well as the influence of interface texturing on interface and bulk material properties. From these, an optically and electronically optimized light management scheme is derived and a horizon for the power conversion efficiency of textured LPC silicon thin-film solar cells on glass is given.

II. Experimental and Numerical Methods

A. Sample Preparation

Liquid phase crystallized silicon thin-film solar cells on glass substrates were produced with a planar interlayer stack consisting of a 250 nm thick silicon oxide (SiO_x)/60 nm silicon nitride (SiN_x)/10nm silicon oxy-nitride (Si(ON)) serving as diffusion barrier, anti-reflective coating, and diffusion and wetting layer, respectively, between glass substrate and silicon absorber [1], [9]. Additionally to this planar reference interlayer stack, two interlayer textures were investigated in this study, namely a sinusoidal texture [7] and a smooth anti-reflective three-dimensional (SMART) texture [8]. The hexagonal sinusoidal texture exhibits a period of 750 nm and a height-to-period ratio of 0.5 and is produced by combining nano-imprint lithography into a commercially available organic resist with reactive ion etching to replicate the texture in the SiO_x diffusion barrier [10]. SiN_x/Si(ON) interlayers were subsequently deposited on the sinusoidal texture. For the

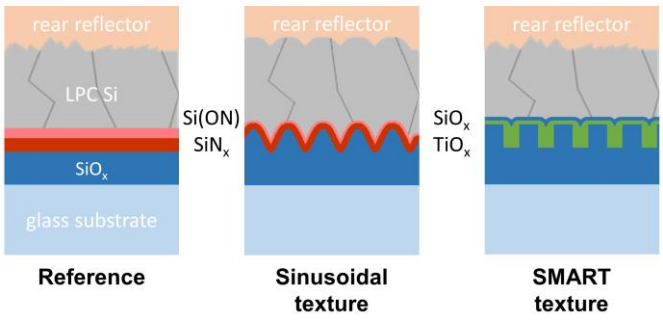

Fig. 1. Schematic sample stacks of the samples investigated (not to scale).

SMART texture, a hexagonal nano-pillar array with a period of 750 nm and height of ~60 nm replicated in high-temperature stable sol-gel and subsequently smoothed by spin-coating of a titanium oxide (TiO_x) precursor solution. Thermal annealing for 30 min at 800 °C results in a compact crystalline TiO_x layer, substituting the silicon nitride anti-reflective coating. The spin-coated TiO_x preferably fills the voids between the nano-pillars, leading to an "optically rough" texture with a morphologically smooth surface. A 10 nm thick SiO_x layer is employed as wetting and diffusion barrier. All samples were coated with 15 µm thick silicon absorbers by electron-beam evaporation, followed by a 100 nm thick SiO_x capping layer.

Liquid phase crystallization is performed using a line-shaped laser with a width of 5 cm and a wavelength of 808 nm. Rapid thermal annealing for 1 min at 950 °C after LPC reduces thermal stress in the glass substrate. The capping layer is removed by wet-chemical etching in a buffered oxide etch solution for 9 min. The top ~300 nm of the LPC silicon layer is etched away in a silicon etching solution consisting of a hydrous solution of hydrofluoric acid, nitric acid and phosphorous acid for 1 min. While the sinusoidal texture exhibits a double-sided texturing due to the usage of a capping layer [11], a random pyramid back-side texture is introduced for the reference and SMART texture samples by wet-chemical etching in an IPA-free solution containing potassium hydroxide (Alkatex free provided by GP Solar) for 3 min at 80 °C. For the SMART texture, an additional sample with Si(ON) passivation layer is produced by solid phase crystallization for 20 h at 600 °C, as so far no successful liquid phase crystallization was feasible using this interlayer combination. Solar cells were produced using the lithography-free contacting scheme introduced by Haschke et al. [12], therein denoted as test cells. All samples were equipped with a white-paint rear reflector. Figure 1 schematically illustrates the samples investigated. Absorptance measurements were performed using a Perkin Elmer Lambda 1050 photo-spectrometer holding the samples in the center of an integrating sphere with a diameter of 15 cm. External quantum efficiency is measured using a home-made set-up with a spot size of 3 × 2 mm^2. Atomic force microscope images used as input for simulations were obtained using a Park Systems XE-70.

B. Simulations

One-dimensional simulations were carried out using the optical simulation software "GenPro4" developed at Delft University of Technology [13]. The software code numerically calculates the absorptance in a layer stack based on the transfer matrix method. Textured interfaces can be treated despite the one-dimensional simulation approach by the implementation of a ray tracing and scalar scattering model [14]. The ray tracing model is employed for the random pyramid texture, for which surface topography data determined by atomic force microscope measurements were used as input. Refractive indices of the layers were taken from literature in case of crystalline silicon [15] or measured by spectroscopic ellipsometry.

III. Results

A. Loss Analysis of Planar LPC Silicon Absorbers

In order to assess the potential of textures at the glass-silicon interface to reduce optical losses in LPC silicon solar cells on glass, losses of the planar state-of-the-art device design were identified as a first step. Figure 2 depicts the measured absorptance in a 15 µm thick LPC silicon absorber (black curve) as well as the calculated absorptance (grey area) from one-dimensional simulations. The curves match well, with only minor deviations for wavelengths > 400 nm, which are attributed to inaccuracies in modelling and, supposedly, defect absorption in the long wavelength range of the real structure. In the short wavelength range up to 400nm, absorptance of the measured sample rises due to parasitic absorption in the glass substrate, which had not been considered in the simulations.

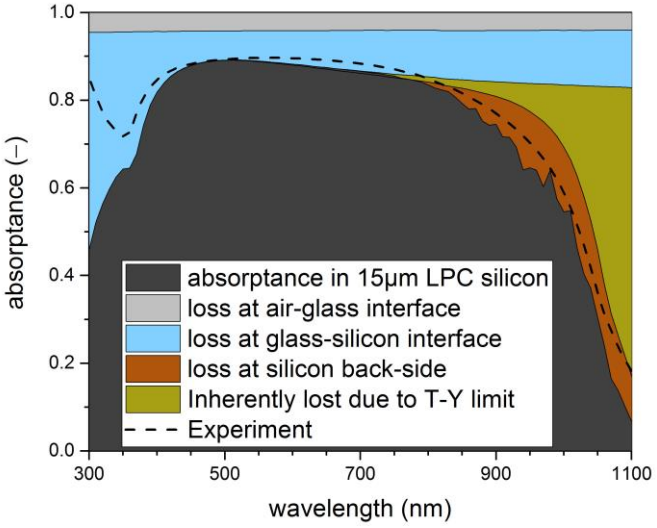

Fig. 2. Absorptance in 15 µm thick LPC silicon from measurement (black dashed line) and one-dimensional simulations (grey area). Losses stemming from the air-glass interface (light grey), glass-silicon interface (blue) and silicon back-side (brown) are displayed. Losses related to the Tiedje-Yablonovitch (T-Y) limit for a 15 µm thick silicon layer considering reflectance at the air-glass and glass-silicon interface are included for reference (dark yellow area).

One-dimensional simulations allow to easily adapt the structure under consideration. In particular, specific interfaces can be "switched off", e.g. neglecting the rear-side of the silicon absorber by assuming an infinitely thick absorber. In doing so, losses can be attributed to a specific interface, as illustrated by differently colored areas in Fig. 2. The air-glass interface (light grey area) causes a loss of around 4 % of the

incoming light independent of wavelength. This amounts to an equivalent maximum achievable short-circuit current density loss of 1.8 mA cm^{-2}. The glass-silicon interface (blue area) has a minimum reflectance of around 6 % at a wavelength of 500 nm. For longer wavelength, reflectance slowly increases up to 15 % for 1100 nm. In the short wavelength range, a steep increase to around 50 % is observed. In total, an equivalent of 4.5 mA cm^{-2} is reflected at this interface. The rear interface only plays a role for wavelengths > 700 nm, for which the penetration depth of the incoming light becomes larger than the absorber thickness. Due to the relatively low absorption coefficient of silicon in the near infrared, a large proportion of the incident light is lost due to non-absorption after passing through the absorber. As a benchmark for light trapping, the Tiedje-Yablonovitch limit [16] for a 15 µm thick silicon layer considering reflectance at the air-glass and glass-silicon interface (dark yellow area) is included in Fig. 2. In this limit, non-absorption steeply rises for wavelengths > 900 nm and an equivalent of 3.4 mA cm^{-2} is lost. Hence, optical losses arising from the rear-side of the silicon layer amount to 0.9 mA cm^{-2} (brown area) if the limitations imposed by the Tiedje-Yablonovitch limit are considered.

Overall, the current device design of LPC silicon thin-film solar cells on glass leads to losses of the maximum achievable short-circuit current density of 7.1 mA cm^{-2} compared to the Tiedje-Yablonovitch limit for 15 µm silicon. Of these, 4.5 mA cm^{-2} can be attributed to the planar glass-silicon interface, proving the necessity of interface textures at this interface.

B. Loss Analysis of Textured LPC Silicon Absorbers

Both, the sinusoidal texture [7], [10] and SMART texture, [8] have demonstrated improved light in-coupling into the silicon absorber. Figure 3 exhibits the absorptance of 15 µm thick LPC silicon absorbers with a planar glass-silicon interface (black), a sinusoidal texture (red) and a SMART texture (green). For the SMART texture, two passivation layers were employed, namely silicon oxide (solid curve) and silicon oxy-nitride (dashed). The analysis of the sample with Si(ON) passivation is restricted to the wavelength range 300 nm – 600 nm to exclude effects from the flat back-side of the SPC silicon sample. Reflectance at the air-glass interface (grey area) and the Tiedje-Yablonovitch limit considering reflectance at the air-glass interface (T-Y limit*(1-R)$_{air-glass}$, dotted) are added for reference to constitute a benchmark for reflectance at the glass-silicon interface.

Both textures efficiently improve anti-reflective properties of LPC silicon absorbers on glass. Comparing the passivation layers for the SMART texture reveal the influence of the 10 nm thin top layer on optical properties. The silicon oxide layer causes an increased reflectance in the short-wavelength range due to its lower refractive index. The SMART texture has a minimum reflectance of 5 % at 650 nm, of which 4 % are reflected at the air-glass interface. For the reference sample, a

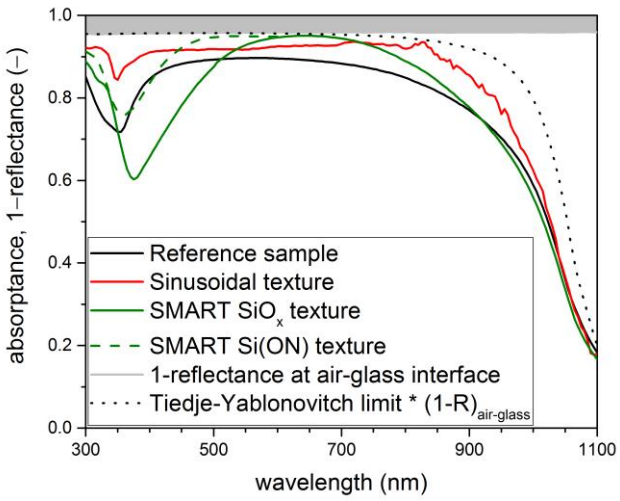

Fig. 3. Absorptance in 15 µm thick LPC silicon absorbers with a planar glass-silicon interface (black), exhibiting a sinusoidal texture (red), and a SMART texture (green). For the SMART texture, both a silicon oxide (SiO_x, solid curve) and silicon oxy-nitride (Si(ON), dashed) passivation layer is depicted. Reflectance at the air-glass interface represented as 1-R (grey area) and Tiedje-Yablonovitch limit after glass reflectance (dotted) is added for reference.

minimum reflectance of 10 % is found. While the sinusoidal texture exhibits a maximum of 7 % reflectance, it provides broader anti-reflective properties compared to the SMART texture, minimizing reflectance in the wavelengths range 300 nm - 400 nm and 750 nm - 1000 nm. Total losses compared to the solar irradiance of the textured samples amount to 7.2 mA cm^{-2} and 8.9 mA cm^{-2} for the LPC silicon absorber with a sinusoidal texture and SMART texture with SiO_x passivation layer, respectively.

Replacing the SiO_x passivation layer with Si(ON) in an LPC absorber is expected to reduce losses in the SMART texture devices by an additional 1.0 mA cm^{-2} due to lower reflectance in the short wavelength range. Thus, total losses of 7.9 mA cm^{-2} may be reached for SMART textured LPC devices with Si(ON) passivation layer. Of these losses, 1.8 mA cm^{-2} are reflected at the air-glass interface and 3.4 mA cm^{-2} are inherently lost, as calculated from the Tiedje-Yablonovitch limit. Hence, the textured glass-silicon interface cause losses of 2.0 mA cm^{-2} and 2.7 mA cm^{-2}, a 56 % and 40 % relative gain compared to the state-of-the-art device design for the sinusoidal and SMART texture with Si(ON) passivation layer.

C. External Quantum Efficiency

Improved light management arising from interface texturing will only lead to an efficiency enhancement if the texture does not affect interface or bulk material quality of the solar cell.

Hence, measurements of the external quantum efficiency (EQE) were performed to further analyze the potential of textures at the glass-silicon interface of LPC silicon thin-film solar cells on glass. Internal quantum efficiency (IQE) was

calculated from absorptance and external quantum efficiency measurements. Figure 4 displays the EQE (solid) and IQE (dashed) of LPC silicon solar cells with a planar glass-silicon interface (black), a sinusoidal texture (red) and a SMART texture with SiO_x passivation layer (green). The reference sample exhibits an EQE of approximately 80 % in the wavelength range from 400 nm to 800 nm, corresponding to an IQE of 90 %. For longer wavelengths, EQE drops in line with absorptance.

For the solar cell with a SMART texture, IQE is slightly lower compared to the solar cell with planar glass-silicon interface.

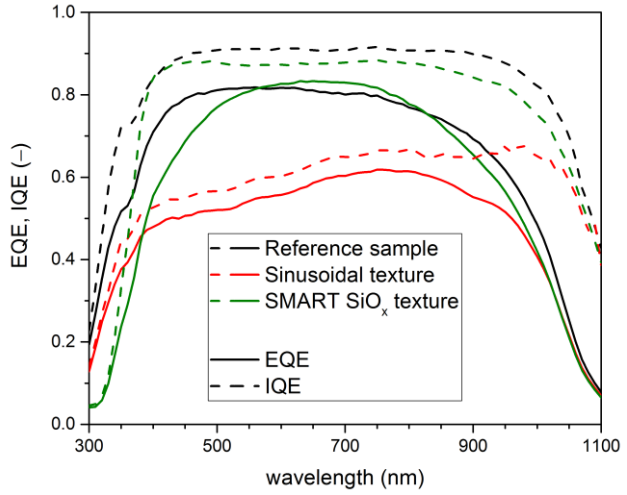

Fig. 4. External (solid) and internal (dashed) quantum efficiency (solid) of LPC silicon solar cells with a planar glass-silicon interface (black), exhibiting a sinusoidal texture (red), and a SMART texture with SiO_x passivation layer (green).

This may be explained by a lower passivation quality provided by the interlayer stack, in particular the silicon oxide passivation layer compared to its silicon oxy-nitride counterpart. Nonetheless, an IQE exceeding 80 % is achieved for the solar cell produced on a SMART textured substrate. EQE of the sample with a sinusoidal texture with height-to-period ratio of 0.5, on the contrary, reveals an inferior EQE and IQE limited to values below 70 %. This is attributed to interface defects induced by the texture occurring despite the optimized interlayer stack that demonstrated surface recombination velocities as low as 200 cm s^{-1} for planar devices [1].

IV. Discussion and Conclusion

Liquid phase crystallized silicon thin-film absorbers were analyzed in regards to their optical properties. One-dimensional simulations allow to differentiate losses stemming from different interfaces in the device. The glass-silicon interface could thereby be identified as the most important one, with a loss of 4.5 mA cm^{-2} out of 7.1 mA cm^{-2} compared to the Tiedje-Yablonovitch limit for a 15 µm thick silicon layer. Losses caused by the air-glass interface and silicon back-side amount to 1.8 mA cm^{-2} and 0.8 mA cm^{-2}, respectively.

Sinusoidal textures and SMART textures were implemented at the glass-silicon interface to mitigate these losses. For the SMART texture, two passivation layers were investigated. Employing these measures, the losses at this interface were reduced from 4.5 mA cm^{-2} for a planar interlayer stack to 2.0 mA cm^{-2} for a sinusoidal texture with height-to-period ratio of 0.5, and 3.7 mA cm^{-2} and 2.7 mA cm^{-2} for a SMART texture with silicon oxide and with silicon oxy-nitride passivation layer, respectively.

Internal quantum efficiencies well above 80 % were measured on solar cells with a planar interlayer stack and SMART texture with silicon oxide passivation layer. For the sinusoidal nano-texture, a detrimental effect on interface and bulk material quality lead to a reduction of IQE to below 70 %. Consequently, the most promising light management scheme combining both, improved optical properties and interface and bulk properties equivalent to devices with planar glass-silicon interface, comprises a SMART texture at the glass-silicon interface and a random pyramid texture at the rear side of the absorber produced by wet-chemical etching in KOH. To fully exploit the optical potential of the SMART texture, it requires to be combined with a silicon oxy-nitride passivation layer. In addition, anti-reflective measures at the air-glass interface, e.g. a moth-eye texture, may contribute to reducing optical losses by reducing reflectance from 4 % to less than 1%. In terms of short-circuit current density, losses at this interface may thereby be lowered to 0.4 mA cm^{-2}.

Combining all these measures, maximum achievable short-circuit current density may be enhanced from 33.4 mA cm^{-2} to 36.8 mA cm^{-2}. Assuming an IQE of 0.9, a short-circuit current density of 33.4 mA cm^{-2} is feasible. If this may be combined with an open-circuit voltage and fill factor already reached on individual solar cells to 670 mV and 79 %, respectively, a power conversion efficiency of 18 % is feasible for LPC silicon thin-film solar cells on glass.

Acknowledgement

The German ministry of education and research (BMBF) is acknowledged for funding the research activities of the Young Investigator Group ‘Nano-SIPPE’ at HZB in the program NanoMatFutur (no. 03X5520). The authors thank Dr. Klaus Jäger and Dr. Daniel Amkreutz for fruitful discussions. GP Solar is acknowledged for providing the Alkatex IPA-free texturing agent.

References

[1] C. Thi Trinh *et al.*, “Potential of interdigitated back-contact silicon heterojunction solar cells for liquid phase crystallized silicon on glass with efficiency above 14%,” *Sol. Energy Mater. Sol. Cells*, vol. 174, no. June 2017, pp. 187–195, 2018.

[2] J. Benick *et al.*, "High-Efficiency n-Type HP mc Silicon Solar Cells," *IEEE J. Photovoltaics*, vol. 7, no. 5, pp. 1171–1175, 2017.

[3] M. Z. Pakhuruddin, J. Dore, J. Huang, and S. Varlamov, "Effects of front and rear texturing on absorption enhancement in laser-crystallized silicon thin-films on glass," *Jpn. J. Appl. Phys.*, vol. 54, p. 08KB04, 2015.

[4] M. Z. Pakhuruddin, J. Huang, J. Dore, and S. Varlamov, "Enhanced light-trapping in laser-crystallised silicon thin-film solar cells on glass by optimised back surface reflectors," *Sol. Energy*, vol. 150, pp. 477–484, 2017.

[5] G. Köppel *et al.*, "Periodic and Random Substrate Textures for Liquid-Phase Crystallized Silicon Thin-Film Solar Cells," *IEEE J. Photovoltaics*, vol. 7, no. 1, pp. 85–90, 2017.

[6] V. Preidel, D. Amkreutz, J. Haschke, M. Wollgarten, B. Rech, and C. Becker, "Balance of optical, structural, and electrical properties of textured liquid phase crystallized Si solar cells," *J. Appl. Phys.*, vol. 117, p. 225306, 2015.

[7] G. Köppel, B. Rech, and C. Becker, "Sinusoidal nanotextures for light management in silicon thin-film solar cells," *Nanoscale*, vol. 8, no. 16, pp. 8722–8728, 2016.

[8] D. Eisenhauer *et al.*, "Smooth anti-reflective three-dimensional textures for liquid phase crystallized silicon thin-film solar cells on glass," *Sci. Rep.*, vol. 7, p. 2658, 2017.

[9] N. Preissler *et al.*, "Impact of Dielectric Layers on Liquid-Phase Crystallized Silicon Solar Cells," *IEEE J. Photovoltaics*, vol. 8, no. 1, pp. 30–37, 2018.

[10] D. Eisenhauer, G. Köppel, B. Rech, and C. Becker, "Improved light management in crystalline silicon thin-film solar cells by advanced nano-texture fabrication," in *Light, Energy and the Environment*, 2017, p. PW2A.4.

[11] C. Becker, V. Preidel, D. Amkreutz, J. Haschke, and B. Rech, "Double-side textured liquid phase crystallized silicon thin-film solar cells on imprinted glass," *Sol. Energy Mater. Sol. Cells*, vol. 135, pp. 2–7, 2015.

[12] J. Haschke, D. Amkreutz, L. Korte, F. Ruske, and B. Rech, "Towards wafer quality crystalline silicon thin-film solar cells on glass," *Sol. Energy Mater. Sol. Cells*, vol. 128, pp. 190–197, 2014.

[13] R. Santbergen, A. H. M. Smets, and M. Zeman, "Optical model for multilayer structures with coherent, partly coherent and incoherent layers.," *Opt. Express*, vol. 21, pp. A262–A267, 2013.

[14] K. Jäger, M. Fischer, R. A. C. M. M. Van Swaaij, and M. Zeman, "A scattering model for nano-textured interfaces and its application in opto-electrical simulations of thin-film silicon solar cells," *J. Appl. Phys.*, vol. 111, no. 8, 2012.

[15] M. A. Green, "Self-consistent optical parameters of intrinsic silicon at 300 K including temperature coefficients," *Sol. Energy Mater. Sol. Cells*, vol. 92, no. 11, pp. 1305–1310, Nov. 2008.

[16] T. Tiedje, E. Yablonovitch, G. D. Cody, and B. G. Brooks, "Limiting efficiency of silicon solar cells," *IEEE Trans. Electron Devices*, vol. 31, no. 5, pp. 711–716, 1984.